Confocal XANES and the Attic Black Glaze: The Three Stage Firing Process through Modern Reproduction

Dr. Lars Lühl[*1,§], *Dr. Bernhard Hesse*[1,$], *Dr. Ioanna Mantouvalou*[1], *Dr. Max Wilke*[2], *Sammia Mahlkow*[1], *Eleni Aloupi-Siotis*[3] *and Prof. Dr. Birgit Kanngießer*[1]

[1] Technische Universität Berlin, Berlin, Germany

[2] Deutsches Geoforschungszentrum, Potsdam, Germany

[3] Thetis Authentics Ltd, Athens, Greece

The decorated black- and red-figured Athenian vases (6th and 5th century BC) and the plain black glazed ware represent a milestone in our material culture due to their aesthetic and technological value; the Attic black glaze is of particular interest since it is a highly resistant potash-alumino-silicate glass, coloured by magnetite nanocrystals (< 200 nm). The study presents a new methodological approach for correlating the iron oxidation state in the black glaze layer with the manufacturing process by means of conventional and confocal X-ray absorption near edge spectroscopy (XANES). The enhanced surface sensitivity of confocal XANES is combined with conventional XANES resulting in higher counting rates in order to reliably evaluate the iron oxidation state (Fe3+/ΣFe) of the surface layer. A detailed description of the new evaluation procedure is given. The 3-stage firing process was retraced by correlating selected attic black glazed (BG) specimens from different periods (Archaic,

Classical, Hellenistic) with laboratory reproductions. The modern BG specimens serving as reference samples, were produced by following the 3-stage firing process (i.e. under oxidizing-reducing-oxidizing (ORO) conditions) at different top temperatures, using clay suspensions of different particle size produced with treatment of raw illitic clays from Attica.

Normalization and background correction

XANES-spectra are normalized by subtracting a quadratic polynomial, which is fitted to the region before the pre-edge (7007-7107 eV) with a fixed quadratic fraction c**.** The shape of the higher energy part is matched to the form of the spectrum by adjusting the quadratic fraction c by hand in the same way as Wilke did it for reference samples to ensure a comparable way of analysis.

The normalization procedure is illustrated in **Fig. S-1**, the grey lines are fitted with different quadratic fractions c to the measured data (black). For $c=1.35*10^{11}$ the fit was subtracted from the measured spectrum revealing the red spectrum. The mean value in the extended region (7177 to 7407 eV) is the blue dashed line, by which the whole red spectrum is divided afterwards. The pre-edge region is closely after the fitted region and, thus, is not influenced by small variations in c.

For spectra measured during the same series of experiments c is found to be similar. In our first set of experiments c varied between $1.2*10^{11}$ and $1.7*10^{11}$, whereas for the second set it varied between $4.1*10^{10}$ and $6.7*10^{10}$ for similar counting rates, due to differences in the alignment. The value of c becomes negative for spectra that show decreasing intensity in the EXAFS region. This can be seen by the ochre spectrum in **Fig. 1** of the reconstruction of the confocal Micro-XANES measurement, which descends in the EXAFS region in the same way as the atomic photo-ionization cross section.

After normalization, the pre-edge region is corrected for the background by fitting the tail of of Gaussian functions using only the data at 7106 to 7110 eV) and 7116 to 7118 eV), and subtracting them from the data. This is shown in **Fig. S-2**, where the squares represent the normalized pre-edge region. The data indicated by the red squares is fitted by two Gaussian functions (grey dashed lines) and the sum of both (grey solid line) is subtracted, revealing the background corrected spectrum (triangles).

As explained in the publication, the background subtracted pre-edge is plotted by two Gaussian functions as shown in **Fig. S-3**. The centroid position and the integrated Area of the pre-edge is determined by the area weighted centroid positions and the areas of the single Gaussian distributions with equation (1) in the main text.

Setup

The most important details of the setup with 7-element detector and position of the polycapillary halflenses can be seen in **Fig. S-4**.

Centroid positions

The centroid positions used for the calculation of the Fe^{3+} amount are given in **Table S-1**. For some of the samples the centroid position were calculated by pseudo-Voigt and Gaussian distributions. This was done, because for the analysis of the reference materials with iron in mineral by Wilke et al. pseudo-Voigt functions where used and for iron in glass gauss functions. Nevertheless, as the R^2 values indicate, for our samples gauss functions always reflect the measured spectra better than the pseudo-Voigt ones.

Figures and Tables

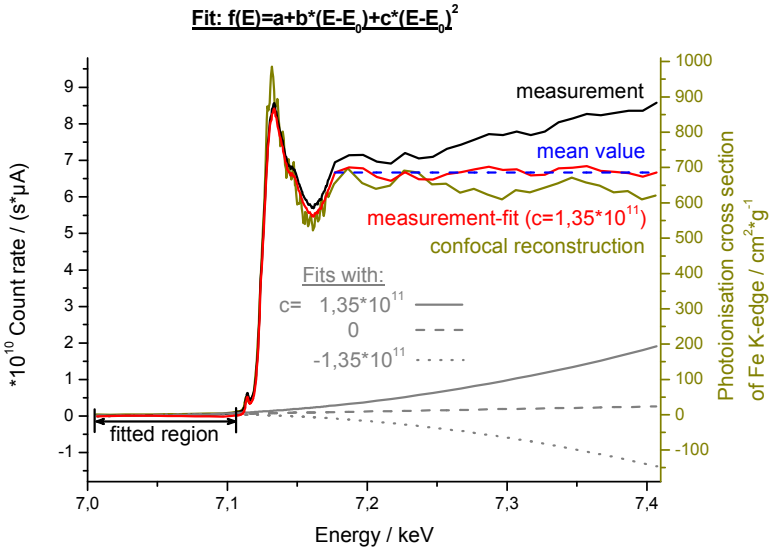

Fig. S-1: Normalization procedure of a measured conventional spectrum (black) fitted with a quadratic polynomial with different quadratic fractions c (grey). For $c=1.35*10^{11}$ the difference of measured spectrum and fit is plotted in red. Afterwards the spectrum is divided by the mean value of the EXAFS-signal (blue). The reconstruction of the confocal spectrum (ochre) is fitted to the right scale.

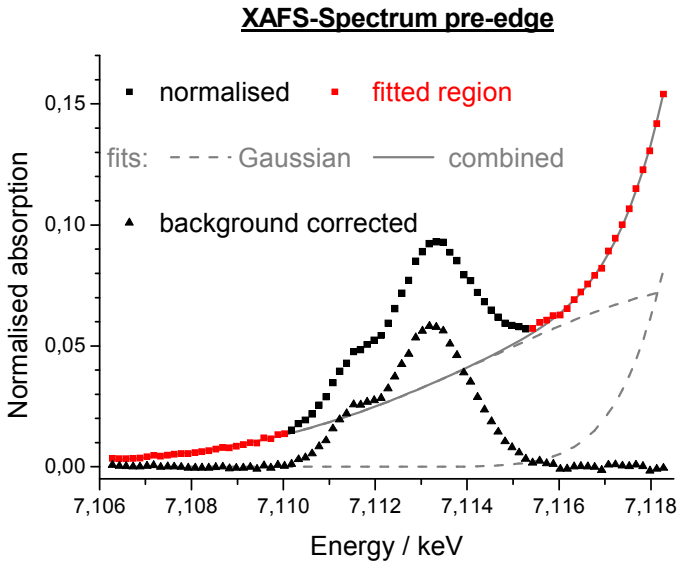

Fig. S-2: Background correction procedure for normalized pre-edges (squares). The regions before and after the pre-edge (red squares) are fitted by two small energy extensions of Gaussian functions (grey dashed) and the sum of both (grey solid) is subtracted revealing the

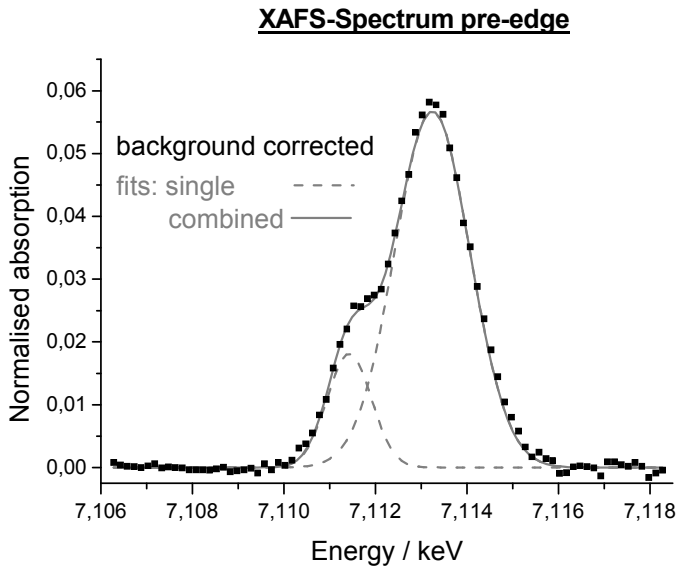

background corrected pre-edge (triangles).

Fig. S-3: Extraction procedure of integrated intensity and centroid position of background corrected pre-edges (squares). Two Gaussian functions i (grey dashed) are fitted to the pre-edge and their areas A_i and centroid positions C_i are used to determine integrated intensity A and centroid position C of the pre-edge according to equation (1).

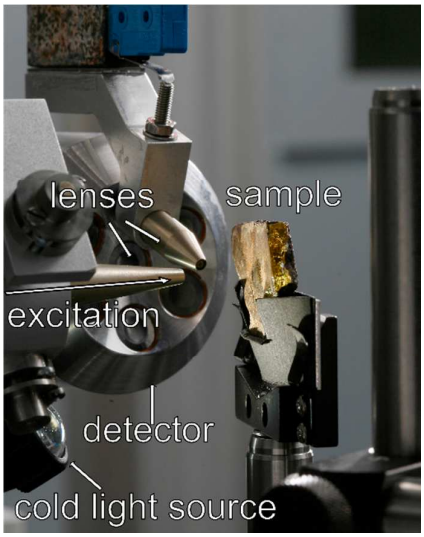

Fig. S-4: Image of the setup where the sample is excited by a focused beam (left lens) and fluorescence intensity is detected by seven detector elements. The confocal detection occurs at the topmost element where a polycapillary lens is placed.

Table S-1: Calculated centroid positions by means of two Gaussian or two pseudo Voigt functions with respective R^2 values for all conventional and four confocal measurements.

BG Sherd						
			Gauss		Pseudo-Voigt	
Coarseness	**Temperature**		**R2**	**Centroid / keV**	**R2**	**Centroid / keV**
A (<0.3 µm)	raw material	1	0.99847	**7.11346**	0.98888	**7.11367**
		2	0.99883	**7.11348**		
	890° C	1	0.99931	**7.11260**	0.99060	**7.11272**
	930° C	1	0.99956	**7.11288**	0.99455	**7.11293**
		1 confocal	0.99688	**7.11293**		
		2	0.99950	**7.11301**	0.99289	**7.11306**
B (<0.8 µm)	870° C	1	0.99924	**7.11326**	0.99365	**7.11343**

		2	0.99881	**7.11330**	0.99386	**7.11339**
		3	0.99945	**7.11298**	0.99517	**7.11296**
	890° C	1	0.99947	**7.11259**	0.99467	**7.11255**
		2	0.99844	**7.11297**	0.97826	**7.11288**
		3	0.99943	**7.11262**	0.99517	**7.11267**
	930° C	1	0.99956	**7.11304**	0.99271	**7.11302**
		1 confocal	0.99316	**7.11301**		
		2	0.99924	**7.11287**	0.99165	**7.11282**
C (<5.5 μm)	870° C	1	0.99728	**7.11337**	0.99138	**7.11366**
		1 confocal	0.99559	**7.11336**		
		2	0.99931	**7.11352**		
	890° C	1	0.99955	**7.11296**	0.98775	**7.11306**
		1 confocal	0.99687	**7.11285**		
		2	0.99861	**7.11295**		
	930° C	1	0.99963	**7.11289**		
		2	0.99884	**7.11306**	0.98862	**7.11316**
Body		1	0.99341	**7.11344**		
		2	0.99955	**7.11325**	0.97204	**7.11301**
Attic pottery						
Age	**Origin**					
Archaic (6^{th} c. BC)	Acropolis	1	0.99958	**7.11297**		
		2	0.99960	**7.11314**		
Classical (5^{th} c. BC)	Kerameikos	1	0.99958	**7.11247**		
		2	0.99924	**7.11249**		
Hellenistic (4^{th} c. BC)	Acropolis	1	0.99956	**7.11275**		
		2	0.99950	**7.11280**		